

A Facile Synthesis of Catechol-Functionalized Poly(ethylene oxide) Block and Random Copolymers

Kaila M. Mattson,^{1,2} Allegra A. Latimer,^{1,2} Alaina J. McGrath,¹ Nathaniel A. Lynd,¹ Pontus Lundberg,¹ Zachary M. Hudson,¹ Craig J. Hawker^{1,2,3}

¹Materials Research Laboratory, University of California, Santa Barbara, California 93106

²Department of Chemistry and Biochemistry, University of California, Santa Barbara, California 93106

³Materials Department, University of California, Santa Barbara, California 93106

Correspondence to: C. J. Hawker (E-mail: hawker@mrl.ucsb.edu)

Received 9 May 2015; accepted 3 July 2015; published online 31 July 2015

DOI: 10.1002/pola.27749

ABSTRACT: Herein we develop a facile synthetic strategy for the functionalization of well-defined polyether copolymers with control over the number and location of catechol groups. Previously, the functionalization of polyethylene oxide (PEO)-based polymers with catechols has been limited to functionalization of the chain ends only, hampering the synthesis of adhesive and antifouling materials based on this platform. To address this challenge, we describe an efficient and high-yielding route to catechol-functionalized polyethers, which could allow the

effects of polymer architecture, molecular weight, and catechol incorporation on the adhesive properties of surface-anchored PEO to be studied. © 2015 Wiley Periodicals, Inc. *J. Polym. Sci., Part A: Polym. Chem.* **2015**, *53*, 2685–2692

KEYWORDS: adhesion; anionic polymerization; biomimetic; diblock copolymers; functionalization of polymers; polyethers; structure-property relations; synthesis; telechelics

INTRODUCTION Polyethylene oxide (PEO) is used widely as a thickening and lubricating agent in food products, cosmetics, and pharmaceuticals.^{1,2} Its simple chemical structure belies its wide-ranging and versatile properties, including good aqueous and organic solubility, low immunogenicity and toxicity, and large aqueous exclusion volume.^{2,3} These qualities make PEO an attractive candidate for use in polymer surface coatings.^{4–6} Grafted PEO can impart a surface with biological stealth, fouling resistance, and water solubility.^{7–9} Contact lenses, for example, can be coated with PEO to enhance their hydrophilicity and reduce biofouling.^{1,2,7}

Despite its many applications, noncovalent grafting of PEO to a variety of different surfaces has been a challenge, as only chain end groups are available for reaction, and adhesive functional units strong enough to operate in aqueous environments are limited.^{2,3,9}

Functionalization of PEO with multiple catechol units presents a potential solution to this problem. Marine organisms, such as mussels, exploit catechol-modified proteins to adhere to a wide variety of surfaces in mechanically and chemically hostile aqueous environments. In these systems, catechols are introduced through the selective hydroxylation of tyrosine residues to give dihydroxyphenyl alanine (DOPA) units, which

are believed to be at least partially responsible for the impressive binding strength of mussels on submerged surfaces.^{7–10} Furthermore, catechols are exceptionally versatile; not only can they bind to a variety of metals and metal-oxides, such as titania, silica, gold, and iron, but they can also adhere firmly to both biological tissue and bone.^{9,11–15}

While catechols have previously been employed to tether PEO to surfaces,^{8,16–27} their use has been complicated by an inability to vary the number and location of the catechol residues on the polyether backbone. In contrast to mussel foot proteins in which numerous DOPA residues are arrayed along the protein backbone, synthetic PEO-based materials have relied almost exclusively on solitary catechol units at one or both ends of the polymer chain. Additionally, a limited number of reports have described the incorporation of up to four catechol units at a single PEO chain end.^{19,21,23,24} Given the host of applications for surface-anchored PEO, an inexpensive and versatile method that provides control over the number and location of catechol units on a PEO backbone is needed.

PEO/catechol-based materials that more closely mimic adhesive proteins in the number and distribution of catechol units along the backbone would also facilitate fundamental

Additional Supporting Information may be found in the online version of this article.

© 2015 Wiley Periodicals, Inc.

studies on adhesion in aquatic organisms. It is known that catechol incorporation is just one of many factors contributing to mussel adhesion; the binding of synthetic bioinspired adhesives has been shown to depend on pH, polymer molecular weight, and chemical environment.^{13,28–32} However, the degree to which these factors play a role in adhesion has been difficult to evaluate experimentally, and has therefore remained relatively unexplored. A modular synthesis of catechol-functionalized PEO amenable to the preparation of large-scale samples that could facilitate the systematic evaluation of biomimetic adhesive materials is needed. Herein, we present a modular strategy starting from readily available methyl eugenol to imbed protected catecholic moieties at controlled levels within polyether backbones synthesized using anionic polymerization.

EXPERIMENTAL

Materials

All reactions were conducted in oven- or flame-dried glassware under an atmosphere of argon. Unless specified, all chemicals were purchased from Sigma-Aldrich and used as received. *Tris*(pentafluorophenyl)borane (>97.0%), *tert*-butyldimethylsilane (95%), and thioacetic acid (97%) were purchased from Fisher Scientific. Deuterated chloroform (CDCl₃) was obtained from Cambridge Isotope Laboratories, Inc. Allyl glycidyl ether (AGE) was purchased from TCI-America, Inc. Ethylene oxide (EO), benzyl alcohol, potassium naphthalenide, and AGE were purified as described by Lee et al.³³ Tetrahydrofuran (THF) was obtained from a J.C. Meyer dry solvent system immediately before use.

Instrumentation

NMR spectra were recorded on Varian VNMRs 600 MHz or Bruker Avance DMX 500 MHz spectrometers at room temperature. Unless otherwise stated, all ¹H and ¹³C NMR spectra are reported in parts per million (ppm), and were measured relative to the signal for residual chloroform in the deuterated solvent (7.26 ppm and 77.16 ppm, respectively). Thiol-ene reactions were irradiated with a UVP Black Ray UV Bench Lamp XX-15L, which emits 365 nm light at 15W. A Micromass QTOF2 Quadrupole/Time-of-Flight Tandem mass spectrometer was used for high-resolution mass analysis using electrospray ionization (ESI). Gas chromatography (GC) was carried out on a Shimadzu GC-2014 with a Resteck column (SHRXL-5MS) and flame ionization detector (FID). Gel permeation chromatography (GPC) was performed at room temperature using chloroform with 0.25 wt % triethylamine as the mobile phase on a Waters 2695 separation module with a Waters 2414 refractive index (RI) detector and a Waters Alliance HPLC System, 2695 separation module with combined Wyatt DAWN HELEOS-II light scattering/Wyatt Optilab rEX refractive index detectors. Number average molecular weights (M_n) and weight average molecular weights (M_w) were calculated relative to linear polyethylene oxide standards or from light scattering data.

((4-Allyl-1,2-phenylene)bis(oxy))bis(*tert*-butyldimethylsilane) (1)

To a 1000 mL 3-neck round bottom flask equipped with an addition funnel and reflux condenser was added methyl eugenol (50.4 mL, 293 mmol), anhydrous cyclohexane (250 mL, 1.2 M), and *tris*(pentafluorophenyl)borane (6.0 g, 11.7 mmol). The solution was allowed to stir for 15 min to ensure homogeneity. The addition funnel was charged with *tert*-butyldimethylsilane (99.6 mL, 601 mmol), which was added to the reaction dropwise over 4.5 h. The reaction was allowed to stir at room temperature for an additional 48 h, at which point complete conversion was observed by GC analysis. The clear, yellow reaction mixture was passed through a plug of silica gel (CH₂Cl₂ as eluent) and concentrated *in vacuo* to afford pure **1** (108.2 g, 98%) as a clear, colorless liquid. IR (neat) $\tilde{\nu}$ = 2930 (w), 2858 (w), 1577 (w), 1508 (s), 1252 (s), 984 (s), 903 (s), 837 (s), 779 (s) cm⁻¹.

¹H NMR (600 MHz, CDCl₃, δ): 6.78 (d, J = 8.0 Hz, 1H), 6.69 (s, 1H), 6.65 (d, J = 8.1 Hz, 1H), 6.01 – 5.91 (m, 1H), 5.10 – 5.02 (m, 2H), 3.29 (d, J = 6.6 Hz, 2H), 1.02 (s, 18H), 0.22 (s, 12H). ¹³C NMR (151 MHz, CDCl₃, δ): 146.75, 145.18, 137.96, 133.23, 121.64, 121.49, 121.01, 115.49, 77.16, 39.64, 26.15, 18.62, 18.61, –3.91, –3.93. HR-ESI C₂₁H₃₈O₂Si₂ calcd. 378.2410, found 378.2410.

S-(3-(3,4-bis((*tert*-butyldimethylsilyl)oxy)phenyl)propyl) ethanethioate (2)

To a round-bottom flask was added **1** (25.5 g, 67.3 mmol), thioacetic acid (5.2 mL, 73.8 mmol), 2,2-dimethoxy-2-phenylacetophenone (865.7 mg, 3.4 mmol), and anhydrous tetrahydrofuran (10 mL, 14.5 M). The reaction mixture was degassed by three freeze-pump-thaw cycles, backfilled with argon, and irradiated with UV light (λ = 365 nm) for 3 h, or until complete conversion was observed by GC analysis. The solvent was removed *in vacuo* to afford **2** (30.4 g, 99%) as a clear yellow liquid, which was used in the next step without further purification. IR (neat) $\tilde{\nu}$ = 2929 (w), 2857 (w), 1694 (s), 1575 (w), 1509 (s), 1252 (s), 905 (s), 837 (s), 779 (s) cm⁻¹.

¹H NMR (600 MHz, CDCl₃, δ): 6.73 (d, J = 8.0 Hz, 1H), 6.64 (s, 1H), 6.60 (d, J = 8.1 Hz, 1H), 2.86 (t, J = 7.2 Hz, 2H), 2.56 (t, J = 7.5 Hz, 2H), 2.32 (s, 3H), 1.88 – 1.80 (m, 2H), 0.99 (dd, J = 4.7, 1.4 Hz, 18H), 0.19 (dd, J = 4.7, 1.4 Hz, 12H). ¹³C NMR (151 MHz, CDCl₃, δ): 195.54, 146.59, 145.03, 134.23, 121.41, 121.33, 120.95, 77.16, 34.14, 31.23, 30.64, 28.50, 26.05, 18.50, 18.49, –3.98, –4.01. HR-ESI C₂₃H₄₂O₃Si₂S calcd. 454.2393, found 454.2392.

3-(3,4-bis((*tert*-butyldimethylsilyl)oxy)phenyl)propane-1-thiol (3)

To a round bottom flask was added **2** (29.9 g, 67.7 mmol) and MeOH (5 mL, 13.5 M). The mixture was then sparged with argon for 1 h. A degassed, saturated solution of K₂CO₃ in MeOH (10 mL) was added to the reaction via syringe. The resulting mixture was stirred at room temperature for 2.5 h, until TLC analysis (9:1 hexanes:CH₂Cl₂ as eluent) indicated the reaction had reached completion. The reaction was

quenched with a saturated aqueous solution of NH_4Cl (10 mL), diluted with deionized H_2O (50 mL), and extracted with ethyl acetate (3×50 mL). The combined organic extracts were dried over anhydrous MgSO_4 , filtered, and concentrated under reduced pressure. The crude product was purified by silica gel chromatography (9:1 hexanes: CH_2Cl_2 as eluent) to afford **3** (20.9 g, 77%), as a clear yellow liquid. IR (neat) $\tilde{\nu}$ = 2929 (w), 2857 (w), 1575 (w), 1509 (s), 1252 (s), 907 (s), 838 (s), 780 (s) cm^{-1} .

^1H NMR (600 MHz, CDCl_3 , δ): 6.74 (d, J = 8.0 Hz, 1H), 6.65 (s, 1H), 6.61 (d, J = 8.2 Hz, 1H), 2.61 (t, J = 7.4 Hz, 2H), 2.51 (q, J = 6.8 Hz, 2H), 1.89 (p, J = 7.2 Hz, 2H), 1.33 (t, J = 7.8 Hz, 1H), 0.99 (dd, J = 4.0, 1.3 Hz, 18H), 0.20 (dd, J = 4.7, 1.3 Hz, 12H). ^{13}C NMR (151 MHz, CDCl_3 , δ): 146.67, 145.07, 134.41, 121.48, 121.39, 120.99, 35.66, 33.67, 26.11, 23.96, 18.59, 18.57, -3.90, -3.95. HR-ESI $\text{C}_{21}\text{H}_{40}\text{O}_2\text{Si}_2\text{S}$ calcd. 412.2288, found 412.2283.

Representative Procedure for Synthesis of Triblock Copolymers: Preparation of $\text{P}(\text{EO}_{92}\text{-co-AGE}_{11})\text{-b-PEO}_{20\text{k}}\text{-b-P}(\text{EO}_{92}\text{-co-AGE}_{11})$

This procedure is based upon the synthesis of $\text{P}(\text{EO-co-AGE})$ described by Lee et al.³³ Polymerizations were performed in custom five-armed, thick-walled glass reactors fitted with ACE-threads and equipped with glass-coated stir bars. The reactors were fitted with Teflon stoppers, a buret containing anhydrous tetrahydrofuran (THF), a flexible connector attached to a buret containing ethylene oxide (EO) (stored on ice), and a glass column sealed with a 6 mm puresep septum and attached to a Schlenk line with a flexible connector. Reactors were assembled hot, cooled under vacuum, and subsequently purged with argon. PEO macroinitiator (30 g, 1.5 mmol) was added to the reactor via one of the arms under a positive pressure of argon. The reactor was then submitted to several cycles of evacuation followed by argon purge to remove oxygen from the system. THF was added to the reactor via buret until the PEO macroinitiator was completely dissolved. Heating to 40 °C was usually necessary for all solids to go into solution. Titration of PEO with potassium naphthalenide solution (0.3 M in THF) produced potassium alkoxide initiators at both chain ends as indicated by the persistence of a pale green color. Potassium naphthalenide was added via cannula through the 6 mm puresep septum. EO (11 g, 260 mmol) was added to the reactor in one portion by lifting the buret out of the ice and letting the contents drain into the reaction via the connector. Allyl glycidyl ether (AGE) (3.8 g, 33 mmol) was added simultaneously via gas tight syringe. The addition of monomers immediately quenched the green color and the polymerizations were carried out at room temperature for 2 to 3 days. Reactions were quenched with degassed methanol and precipitated from hexanes. The polymer was purified using a plug of silica gel (10% $\text{MeOH}/\text{CH}_2\text{Cl}_2$ as eluent). M_n was determined by ^1H NMR and GPC analysis. PDIs (M_w/M_n) were determined by GPC. M_n = 31.8 kg mol^{-1} ; M_w/M_n = 1.02.

^1H NMR (600 MHz, CDCl_3 , δ): 5.87–5.93 (m), 5.82 (ddt, J = 17.3, 10.7, 5.5 Hz), 5.19 (broad dd, J = 17.3, 1.7 Hz) 5.09 (broad dd, J = 10.3, 1.6 Hz), 4.29 (p, J = 6.8 Hz), 3.92–3.93 (m), 3.41–3.72 (m), 1.49 (dd, J = 17.3, 1.7 Hz). ^{13}C NMR (150 MHz, CDCl_3 , δ): 145.99, 134.80, 116.80, 100.87, 78.39, 72.27, 71.23, 70.82, 70.75, 70.55, 70.15, 69.75, 61.62, 9.22.

$\text{P}(\text{EO}_{101}\text{-co-AGE}_3)\text{-b-PEO}_{20\text{k}}\text{-b-P}(\text{EO}_{101}\text{-co-AGE}_3)$
 M_n = 29.1 kg mol^{-1} ; M_w/M_n = 1.01

$\text{P}(\text{EO}_{98}\text{-co-AGE}_6)\text{-b-PEO}_{20\text{k}}\text{-b-P}(\text{EO}_{98}\text{-co-AGE}_6)$
 M_n = 31.1 kg mol^{-1} ; M_w/M_n = 1.04

$\text{P}(\text{EO}_{92}\text{-co-AGE}_{11})\text{-b-PEO}_{20\text{k}}\text{-b-P}(\text{EO}_{92}\text{-co-AGE}_{11})$
 M_n = 31.8 kg mol^{-1} ; M_w/M_n = 1.02

$\text{P}(\text{EO}_{98}\text{-co-AGE}_6)\text{-b-PEO}_{10\text{k}}\text{-b-P}(\text{EO}_{98}\text{-co-AGE}_6)$
 M_n = 20.0 kg mol^{-1} ; M_w/M_n = 1.03

THP- $\text{PEO}_{10\text{k}}\text{-b-P}(\text{EO}_{98}\text{-co-AGE}_6)$

Synthesis of the diblock copolymer was performed in one pot by sequential monomer addition using 2-(2-hydroxyethoxy) tetrahydropyran (THP) as initiator.

M_n = 14.5 kg mol^{-1} ; M_w/M_n = 1.01

$\text{P}(\text{EO}_{320}\text{-co-AGE}_{28})$

Synthesis of the random copolymer was performed in analogy with the synthesis of the triblocks, using benzyl alcohol as initiator.

M_n = 17.3 kg mol^{-1} ; M_w/M_n = 1.08

Representative Procedure for Thiol-ene Coupling of (3) to Copolymers: Preparation of $\text{P}(\text{EO}_{92}\text{-co-fAGE}_{11})\text{-b-PEO}_{20\text{k}}\text{-b-P}(\text{EO}_{92}\text{-co-fAGE}_{11})$

(fAGE represents catechol-functionalized AGE after thiol-ene coupling). To a round bottom flask was added $\text{P}(\text{EO}_{92}\text{-co-AGE}_{11})\text{-b-PEO}_{20\text{k}}\text{-b-P}(\text{EO}_{92}\text{-co-AGE}_{11})$ (2.1 g, 0.07 mmol, 1.4 mmol alkene), (3) (4.1 g, 9.9 mmol), and anhydrous THF (10 mL). The reaction mixture was degassed by three freeze-pump-thaw cycles, backfilled with argon, and irradiated with UV light (λ = 365 nm) for 4 h, or until complete disappearance of the alkene peaks as indicated by ^1H NMR analysis. The reaction mixture was precipitated from hexanes, filtered, and dried, yielding a white powder. M_n = 45.5 kg mol^{-1} ; M_w/M_n = 1.03.

^1H NMR (600 MHz, CDCl_3 , δ): 6.71 (d, J = 8.0 Hz), 6.63 (s, 1H), 6.60 (d, J = 8.2 Hz), 3.82–3.29 (broad m), 2.60–2.51 (m), 2.47 (t, J = 7.2 Hz), 1.81 (m), 0.97 (d, J = 3.3 Hz), 0.18 (d, J = 3.5 Hz).

$\text{P}(\text{EO}_{101}\text{-co-fAGE}_3)\text{-b-PEO}_{20\text{k}}\text{-b-P}(\text{EO}_{101}\text{-co-fAGE}_3)$
 M_n = 35.2 kg mol^{-1} ; M_w/M_n = 1.01

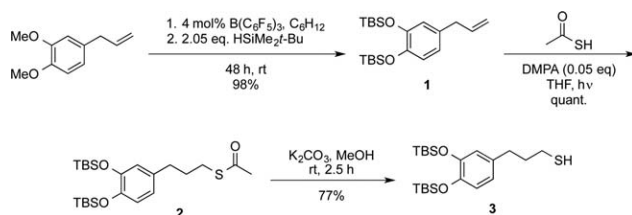
$\text{P}(\text{EO}_{98}\text{-co-fAGE}_6)\text{-b-PEO}_{20\text{k}}\text{-b-P}(\text{EO}_{98}\text{-co-fAGE}_6)$
 M_n = 42.5 kg mol^{-1} ; M_w/M_n = 1.04

$\text{P}(\text{EO}_{92}\text{-co-fAGE}_{11})\text{-b-PEO}_{20\text{k}}\text{-b-P}(\text{EO}_{92}\text{-co-fAGE}_{11})$
 M_n = 45.5 kg mol^{-1} ; M_w/M_n = 1.03

P(EO_{98-co-fAGE}₆)-*b*-PEO_{10k}-*b*-P(EO_{98-co-fAGE}₆) $M_n = 27.6 \text{ kg mol}^{-1}$; $M_w/M_n = 1.05$ **THP-PEO_{10k}-*b*-P(EO_{98-co-fAGE}₆)** $M_n = 18.6 \text{ kg mol}^{-1}$; $M_w/M_n = 1.04$ **P(EO_{320-co-fAGE}₂₈)** $M_n = 29.2 \text{ kg mol}^{-1}$; $M_w/M_n = 1.11$ **RESULTS AND DISCUSSION****"Clickable" Catechols**

In this study, we present a versatile, straightforward, and high-yield synthetic strategy that allows access to a wide variety of well-defined catechol-functionalized polyethers. Key to this strategy is the synthesis of a protected catechol with a thiol functional handle conducive to facile coupling onto polymers with pendent alkenes.

Prior work has highlighted the oxidative instability of catechol units during the multistep functionalization of various materials. When exposed to neutral and basic conditions, the catechol can readily oxidize to its quinone form, which not only substantially decreases its adhesive capabilities but also allows for unwanted cross-linking and addition reactions.^{34,35} For this reason, we sought a robust precursor with a protected catechol functionality. Methyl eugenol, a common phenylpropanoid found in many plants,³⁶ is an ideal starting material because it is both inexpensive and readily available. Direct use of methyl eugenol and methyl ether protection of the eugenol group is not viable as traditional methods for deprotecting methyl ethers can prove challenging, involving harsh conditions incompatible with numerous functional group types.³⁷ For this reason, a hydrosilylation reaction catalyzed by *tris*(pentafluorophenyl)borane ($B(C_6F_5)_3$) was employed to exchange both methyl ether protecting groups with the synthetically more versatile *tert*-butyldimethylsilyl (TBS) groups (Scheme 1). This gives the protected product **1** in 98% yield, which is stable under ambient conditions for extended periods. Radical addition of thioacetic acid across the allyl unit of **1** facilitated installation of an acetyl-protected thiol, **2**. Treatment with mild base selectively cleaves the acetyl protecting group, yielding the desired silyl-protected catechol derivatized with a thiol functional handle **3**. Significantly, the synthesis of **3** from methyl eugenol can be performed efficiently on a large, multi-gram scale and results in an overall yield of 75%.



SCHEME 1 Synthetic strategy for thiol-terminated protected catechol.

Small Molecule Characterization

¹H NMR unambiguously shows the progression from methyl eugenol to the final product **3** (Fig. 1). Briefly, the signature changes include the disappearance of the methyl ether signals ($\delta = 3.82$ ppm) and the corresponding appearance of the *tert*-butyl and dimethyl signals ($\delta = 1.02$ and 0.22 ppm). Quantitative installation of the *S*-acetyl protected thiol **2** is confirmed by the loss of olefin peaks ($\delta = 6.01$ – 5.91 ppm and 5.10 – 5.02 ppm), shifts in the alkyl region, and appearance of the thioacetate methylene singlet ($\delta = 2.32$ ppm). Finally, selective cleavage of the thioacetate group in the presence of TBS is evidenced by the disappearance of the aforementioned thioacetate methylene singlet and emergence of the thiol triplet ($\delta = 1.34$ ppm) with no significant change in the TBS or aromatic regions.

Gas chromatography (GC) further corroborates the success of each reaction shown in Scheme 1 [Fig. 2(a)]. Each intermediate has a distinct and unique GC profile, confirming not only the completeness of the reaction, but also the purity of the product. Crucially, the TBS protecting groups remain intact throughout the protocol and there are no appreciable byproducts (from oxidation, disulfide formation, or otherwise).

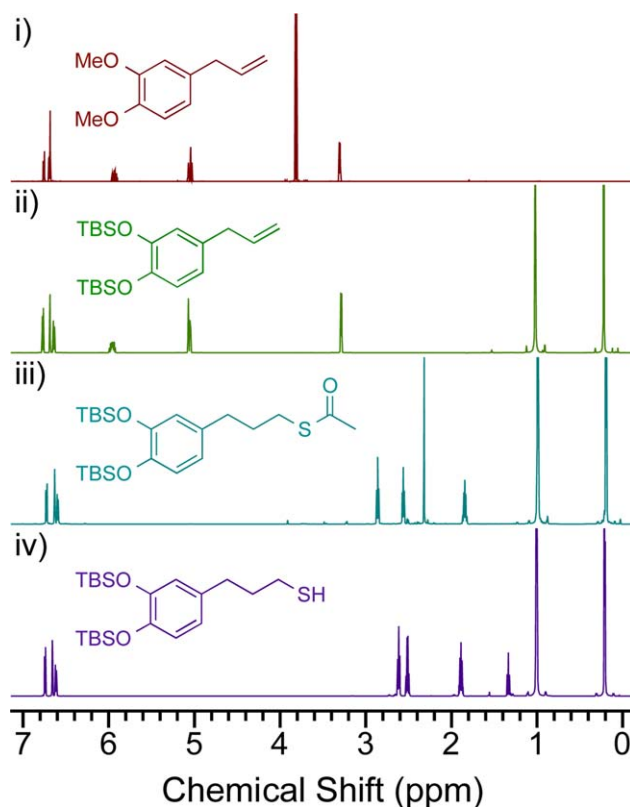


FIGURE 1 ¹H NMR showing the progression from (i) methyl eugenol to (ii) TBS-protected catechol **1**, (iii) thioacetate-terminated catechol **2**, to (iv) the thiol-functionalized protected catechol product **3**.

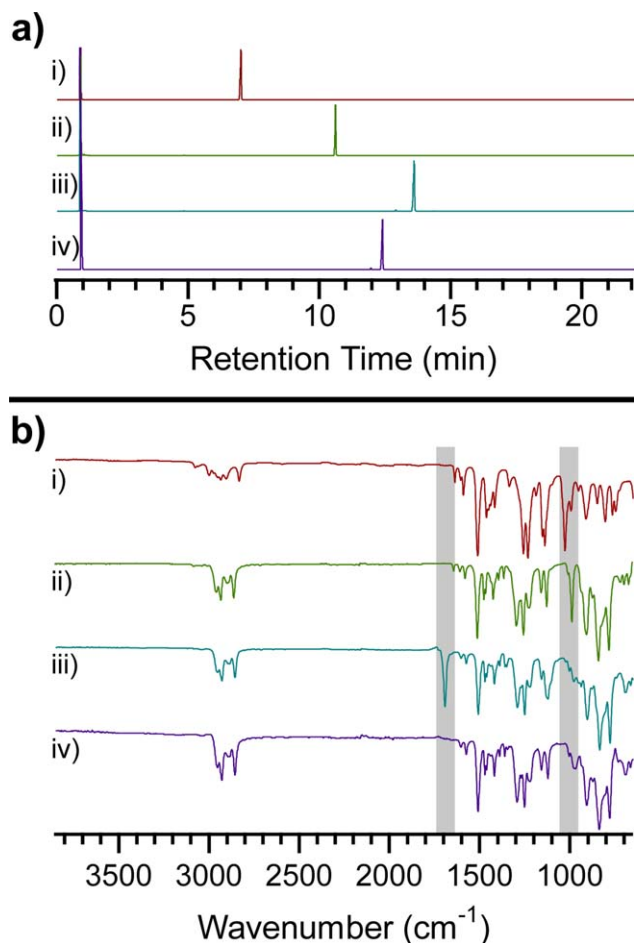


FIGURE 2 (a) Gas chromatograms depicting the progression from (i) starting material methyl eugenol to (ii) TBS-protected intermediate **1**, (iii) *S*-acetyl functionalized **2**, and (iv) silyl-protected thiol-derivatized catechol **3**. The signal at 1 minute is acetone, the solvent used for GC analysis. (b) FT-IR of (i) methyl eugenol, (ii) compound **1**, (iii) **2**, and (iv) **3**. Boxes present to emphasize the signature changes indicative of successful transformation.

Figure 2(b) shows the FT-IR spectra of methyl eugenol and compounds **1-3**. In the top two spectra, a strong alkene signal is clearly visible around 1000 cm^{-1} . This signal is then replaced by the carbonyl signal at 1694 cm^{-1} , indicating incorporation of the thioacetate. Successful cleavage of the *S*-acetyl protecting group is evidenced by the complete disappearance of the aforementioned carbonyl signal.

The design of small molecule **3** was originally inspired by previously published work from our group.³⁸ In that report, triethylsilane (TES) was used to derivatize 4-allyl-2-methoxyphenol, and then reacted with commercially available poly[(mercaptopropyl)methylsiloxane], yielding catechol-functionalized polysiloxanes. Our initial efforts focused on adapting this small-molecule chemistry for polyether functionalization (Supporting Information Scheme S2). After derivatizing the TES-protected catechol, making it amendable to

thiol-ene chemistry (**5**) (initial studies utilized ethane dithiol),³⁹ we then coupled it to a P(EO-*co*-AGE)-*b*-PEO-*b*-P(EO-*co*-AGE) triblock copolymer. Unfortunately, gel permeation chromatography (GPC) showed a dramatic increase in dispersity as well as the formation of a significant amount of high molecular weight byproduct [Fig. 3(a)]. Passing the unfunctionalized polymer through a plug of silica gel before use improved the result; however, the high molecular weight peak persisted [Fig. 3(b)]. We attributed this peak to polymer chain-chain coupling and expended significant efforts probing its origins. The most dramatic improvement [Fig. 3(c)] was realized by replacing the TES protecting groups (**5**) with methoxy groups (**6**), which are neither acid nor base labile (Supporting Information Scheme S3).

The clear improvement shown in Figure 3(c) provided compelling evidence that TES units were too labile. Despite the enhanced performance of **6**, its methyl ethers would be challenging to remove, typically requiring the use of harsh reagents like BBr_3 .³²

It therefore became evident that we needed to explore different protecting groups and synthetic pathways. Through exchange of the TES with TBS protecting groups, the ability to use inexpensive starting materials was maintained by capitalizing upon efficient $\text{B}(\text{C}_6\text{F}_5)_3$ hydrosilylation chemistry. TBS provides enhanced stability compared with TES, yet conveniently remains labile under acidic conditions. This is ideal for exposure of the catecholic moiety, as it decreases the likelihood of catechol oxidation.¹³

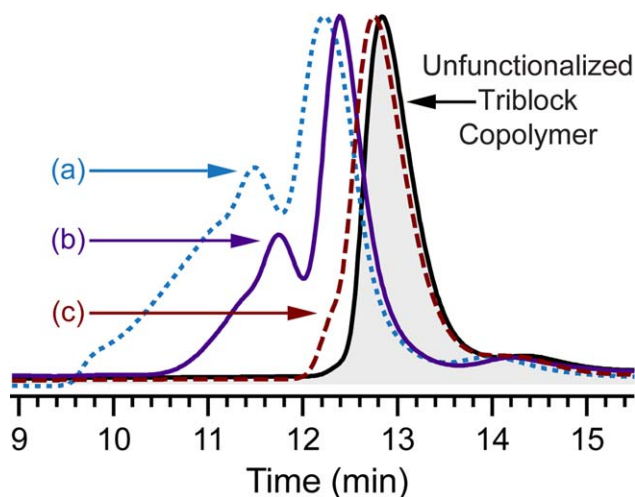
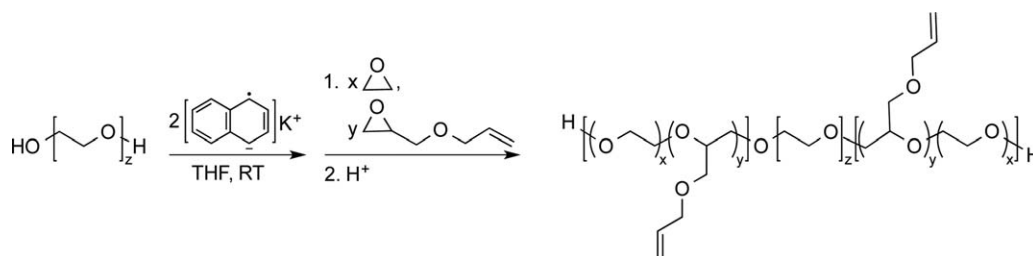


FIGURE 3 GPC traces showing the functionalization of triblock copolymer P(EO₉₈-*co*-AGE₆)-*b*-PEO_{10k}-*b*-P(EO₉₈-*co*-AGE₆) ($M_n = 20.0\text{ kg mol}^{-1}$; $M_w/M_n = 1.03$) using (a) TES-catechol **5** ($M_w/M_n = 3.18$), (b) TES-catechol **5** after passing the starting polymer through a short silica plug ($M_w/M_n = 1.39$), and (c) with methoxy-catechol **6** after passing the starting polymer through a short silica plug ($M_w/M_n = 1.21$). The slight shift retention times results from small daily fluctuations in the instrument.



SCHEME 2 Representative synthesis of P(EO-co-AGE)-b-PEO-b-P(EO-co-AGE) triblock copolymers.

Synthesis and Functionalization of Polyethers

Compared with the previous lack of methods for preparing materials with precise numbers of catechols in a polyether backbone, the mild and quantitative nature of thiol-ene chemistry for polymer functionalization, coupled with the efficient synthesis of **3**, proved ideal. A variety of random, diblock and triblock P(EO-co-AGE) copolymers were therefore synthesized as shown in Scheme 2. For the diblock and triblock P(EO-co-AGE) copolymers, copolymer blocks with varied amounts of AGE were grown from the chain end(s) of commercially available PEO homopolymers by ring-opening anionic polymerization according to Table 1.

The use of AGE allows relative sequence control to be realized in two ways. First, restricting AGE units to certain blocks along the PEO backbone controls the general location of catechol units. The library of polymers synthesized herein includes examples in which catechols are restricted to one or both end-blocks of a polymer chain. Alternatively, starting from a random copolymer allows the catechol units to be distributed along the poly(ethylene oxide) backbone in its entirety.

Examining this further, previous experiments have shown the relative reactivity ratios of EO and AGE monomers in anionic polymerization to be 0.54 and 1.31, respectively.³³ Therefore, an approximate gradient of catechol units in the polymer backbone was naturally achieved through the

copolymerization of EO and AGE. Separately, the number of AGE units incorporated into the PEO backbone can be readily controlled by the initial feed ratio of AGE and EO. This allows the number of catechol units, as well as their distribution, to be precisely controlled.

Polymer Functionalization

The strategy for the post-polymerization functionalization of the P(EO-co-AGE) copolymers and characterization are shown in Figure 4. Thiol-ene chemistry was chosen due to its mild reaction conditions, functional group tolerance, and high efficiency. The thiol-ene addition occurs via radical addition of a thiol across a carbon-carbon double bond.⁴⁰ The reaction proceeds with quantitative yield, as evidenced by complete disappearance of alkene peaks in ¹H NMR [Fig. 4(b)]. Notably, GPC shows no appreciable increase in dispersity after functionalization [Fig. 4(c)].

These results clearly demonstrate successful production of well-defined materials with controlled architecture, catechol incorporation, and catechol placement within the polyether backbone. Deprotection was then accomplished by using a modified literature procedure.⁴¹ In brief, the TBS groups were removed by stirring the polymer in a 1.2 M solution of HCl at 60 °C overnight. Complete disappearance of the TBS peaks in ¹H NMR verifies successful deprotection (Fig. 5).

TABLE 1 PEO-PAGE Copolymers Synthesized and Functionalized with Silyl-Protected Catechols, **3**

No.	Initial PEO Block		Architecture	EO-AGE Copolymer			Catechol-Functionalized Polymer	
	M_n (kg mol ⁻¹) ^a	M_w/M_n ^a		M_n (kg mol ⁻¹) ^a	M_w/M_n ^a	AGE (#) ^b	M_w/M_n ^a	Catechol (#) ^b
1	21.7	1.03	Triblock	29.1	1.01	6	1.01	6
2	21.7	1.03	Triblock	30.1	1.04	12	1.04	12
3	21.7	1.03	Triblock	31.8	1.02	22	1.03	22
4	11.1	1.02	Triblock	20.0	1.03	12	1.05	12
5 ^c	N/A	N/A	Diblock	14.5	1.01	6	1.04	6
6 ^d	N/A	N/A	Random	17.3	1.08	28	1.11	28

^a All values determined by GPC (CHCl₃).

^b Approximate values determined by ¹H NMR and GPC analysis.

^c Diblock analogue was synthesized by sequential monomer addition in one pot.

^d P(EO-co-AGE) random copolymer.

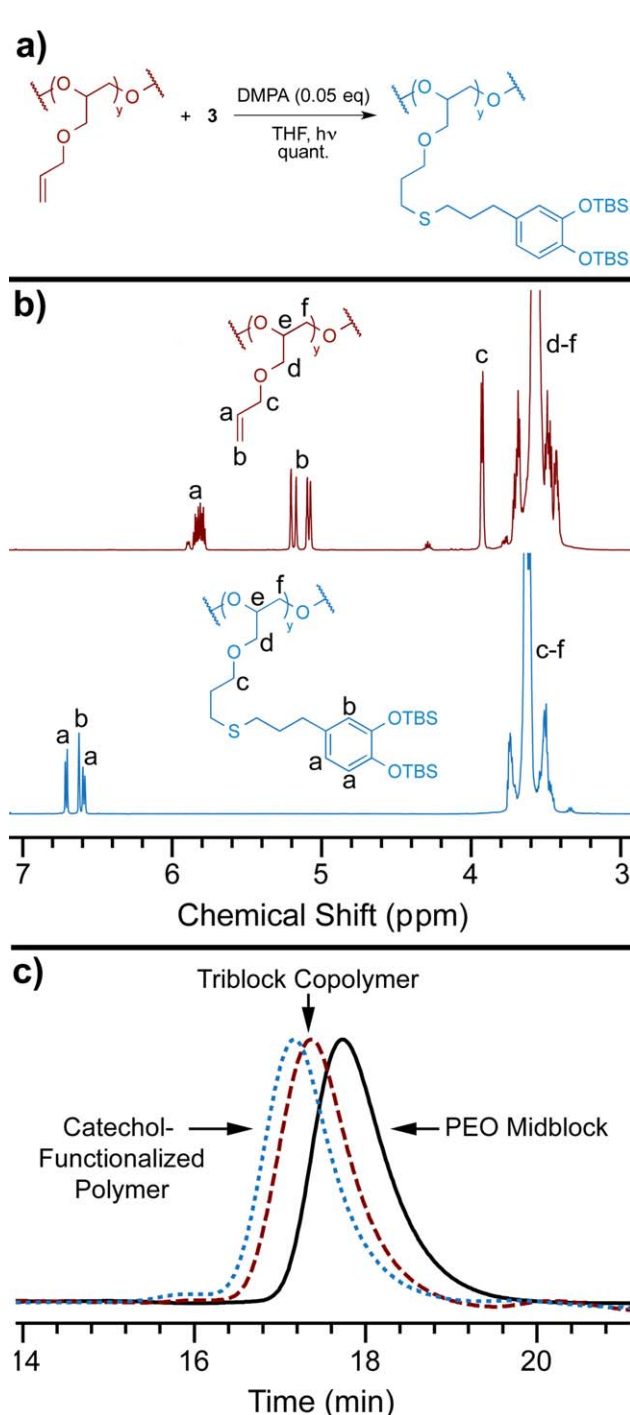


FIGURE 4 (a) Synthetic strategy for polymer functionalization with protected catechol **3**. (b) ¹H NMR spectra showing diagnostic changes before (top) and after (bottom) thiol-ene coupling with **3**. (c) GPC traces of the commercially available PEO midblock (black solid line, $M_n = 21.7 \text{ kg mol}^{-1}$, $M_w/M_n = 1.03$), the P(EO-co-AGE)-*b*-PEO-*b*-P(EO-co-AGE) triblock copolymer synthesized by chain-extending the PEO midblock (red dashed line, $M_n = 31.8 \text{ kg mol}^{-1}$, $M_w/M_n = 1.02$), and the product polymer resulting from quantitative thiol-ene coupling of the AGE units with silyl-protected catechols (blue dotted line, $M_n = 45.5 \text{ kg mol}^{-1}$, $M_w/M_n = 1.03$).

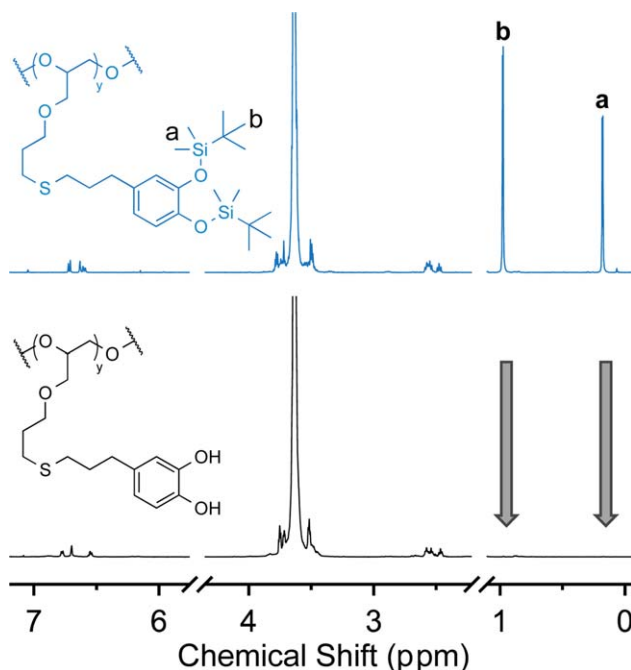


FIGURE 5 ¹H NMR spectra in CDCl₃ showing diagnostic changes before (top) and after (bottom) deprotection of the polyether-tethered catechols. Please note, the spectra have been truncated to emphasize the portions of relevance. The full spectra are available in the SI (Supporting Information Fig. S3).

CONCLUSIONS

We have presented a simple, high-yielding synthesis of tunable catechol-PEO systems. These efforts represent the first time catechols have been controllably dispersed throughout a PEO backbone. Additionally, the low cost of starting materials, minimal purification, and modular nature of this approach represents significant potential for the widespread use of this synthetic strategy. The precise tunability afforded by this system also facilitates systematic investigation of the effects that variables such as molecular weight, catechol incorporation, and catechol location can have on surface-anchored PEO. Finally, this chemistry provides a route to biomimetic adhesive materials that may facilitate future studies into the mechanics of mussel adhesion.

ACKNOWLEDGMENTS

We thank Dr. Christian W. Pester and Professor Ram Seshadri for helpful discussions. This work was supported by the Institute for Collaborative Biotechnologies through grant W911NF-09-0001 from the U.S. Army Research Office (N.A. Lynd and C.J. Hawker) and the UCSB MRSEC Program of the National Science Foundation under award NSF DMR-1121053 (K.M. Mattson, A.A. Latimer, Z.M. Hudson, P. Lundberg and C.J. Hawker). Partial support by the National Institutes of Health as a Program of Excellence in Nanotechnology (HHSN268201000046C) (A.J. McGrath and C.J. Hawker) is also gratefully acknowledged. K.M. Mattson thanks the NSF Graduate Research Fellowship and

ConvEne IGERT Program (NSF-DGE 0801627) for funding. Z.M. Hudson thanks the California NanoSystems Institute for an Elings Prize Fellowship. A.A. Latimer acknowledges support through the Research Internships in Science and Engineering (RISE—UCSB MRSEC) and McNair Scholars Programs. P. Lundberg thanks the Wenner-Gren foundations and Bengt Lundqvist memorial foundation for financial support.

REFERENCES AND NOTES

- 1 C. Fruijtier-Pölloth, *Toxicology* **2005**, *214*, 1–38.
- 2 R. B. Greenwald, Y. H. Choe, J. McGuire, C. D. Conover, *Adv. Drug Deliv. Rev.* **2003**, *55*, 217–250.
- 3 B. Obermeier, F. Wurm, C. Mangold, H. Frey, *Angew. Chem. Int. Ed.* **2011**, *50*, 7988–7997.
- 4 S. J. Sofia, C. Premnath, E. W. Merrill, *Macromolecules* **1998**, *31*, 5059–5070.
- 5 A. Halperin, *Langmuir* **1999**, *15*, 2525–2533.
- 6 (a) R.-V. Ostaci, D. Dameron, Al. S. Akhrass, Y. Grohens, E. Drockenmüller, *Polym. Chem.* **2011**, *2*, 348–354; (b) P. M. Saville, P. A. Reynolds, J. W. White, C. J. Hawker, J. M. J. Frechet, K. L. Wooley, J. Penfold, J. R. P. Webster, *J. Phys. Chem.* **1995**, *99*, 8283–8289.
- 7 K. Knop, R. Hoogenboom, D. Fischer, U. S. Schubert, *Angew. Chem. Int. Ed.* **2010**, *49*, 6288–6308.
- 8 V. S. Wilms, H. Bauer, C. Tonhauser, A.-M. Schilman, M.-C. Müller, W. Tremel, H. Frey, *Biomacromolecules* **2013**, *14*, 193–199.
- 9 (a) B. P. Lee, P. B. Messersmith, J. N. Israelachvili, J. H., Waite, *Annu. Rev. Mater. Res.* **2011**, *41*, 99–132; (b) K. E. Feldman, M. J. Kade, T. F. A. de Greef, E. W. Meijer, E. J. Kramer, C. J. Hawker, *Macromolecules*, **2008**, *41*, 4694–4700.
- 10 J. H. Waite, M. L. Tanzer, *Science* **1981**, *212*, 1038–1040.
- 11 H. J. Meredith, C. L. Jenkins, J. J. Wilker, *Adv. Funct. Mater.* **2014**, *24*, 3259–3267.
- 12 S. Hong, K. Yang, B. Kang, C. Lee, I. T. Song, E. Byun, K. I. Park, S. W. Cho, H. Lee, *Adv. Funct. Mater.* **2013**, *23*, 1774–1780.
- 13 J. Yu, W. Wei, M. S. Menyo, A. Masic, J. H. Waite, J. N. Israelachvili, *Biomacromolecules* **2013**, *14*, 1072–1077.
- 14 G. Bilic, C. Brubaker, P. B. Messersmith, A. S. Mallik, T. M. Quinn, C. Haller, E. Done, L. Gucciardo, S. M. Zeisberger, R. Zimmermann, J. Deprest, A. H. Zisch, *Am. J. Obstet. Gynecol.* **2010**, *202*, 85.e1–85.e9.
- 15 K. J. Winstanley, A. M. Sayer, D. K. Smith, *Org. Biomol. Chem.* **2006**, *4*, 1760–1767.
- 16 B. Mizrahi, X. Khoo, H. H. Chiang, K. J. Sher, R. G. Feldman, J.-J. Lee, S. Irueta, D. S. Kohane, *Langmuir* **2013**, *29*, 10087–10094.
- 17 Y. Ai, Y. Wei, J. Nie, D. Yang, *J. Photochem. Photobiol. B Biol.* **2013**, *120*, 183–190.
- 18 B.-H. Im, J.-H., Jeong, M. R. Haque, D. Y. Lee, C.-H. Ahn, J. E. Kim, Y. Byun, *Biomaterials* **2013**, *34*, 2098–2106.
- 19 S. Mondini, C. Drago, A. M. Ferretti, A. Puglisi, A. Ponti, *Nanotechnology* **2013**, *24*, 105702.
- 20 T. Kotsokechagia, N. M. Zaki, K. Syres, P. De Leonardis, A. Thomas, F. Cellesi, N. Tirelli, *Langmuir* **2012**, *28*, 11490–11501.
- 21 T. Gillich, E. M. Benetti, E. Rakhmatullina, R. Konradi, W. Li, A. Zhang, A. D. Schlüter, M. Textor, *J. Am. Chem. Soc.* **2011**, *133*, 10940–10950.
- 22 C. E. Brubaker, H. Kissler, L.-J. Wang, D. B. Kaufman, P. B. Messersmith, *Biomaterials* **2010**, *31*, 420–427.
- 23 A. Statz, J. Finlay, J. Dalsin, M. Callow, J. A. Callow, P. B. Messersmith, *Biofouling* **2006**, *22*, 391–399.
- 24 J. L. Dalsin, L. Lin, S. Tosatti, J. Vörös, M. Textor, P. B. Messersmith, *Langmuir* **2005**, *21*, 640–646.
- 25 B. P. Lee, J. L. Dalsin, P. B. Messersmith, *Biomacromolecules* **2002**, *3*, 1038–1047.
- 26 J. Sedó, J. Saiz Poseu, F. Busqué, D. Ruiz Molina, *Adv. Mater.* **2013**, *25*, 653–701.
- 27 H. Lee, K. D. Lee, K. B. Pyo, S. Y. Park, H. Lee, *Langmuir* **2010**, *26*, 3790–3793.
- 28 W. Wei, J. Yu, M. A. Gebbie, Y. Tan, N. R. Martinez Rodriguez, J. N. Israelachvili, J. H. Waite, *Langmuir* **2015**, *31*, 1105–1112.
- 29 M. Yu, T. J. Deming, *Macromolecules* **1998**, *31*, 4739–4745.
- 30 V. Ball, D. D. Frari, V. Toniazzo, D. Ruch, *J. Colloid Interface Sci.* **2012**, *386*, 366–372.
- 31 C. R. Matos-Pérez, J. D. White, J. J. Wilker, *J. Am. Chem. Soc.* **2012**, *134*, 9498–9505.
- 32 C. L. Jenkins, H. J. Meredith, J. J. Wilker, *ACS Appl Mater Interfaces* **2013**, *5*, 5091–5096.
- 33 B. F. Lee, M. Wolffs, K. T. Delaney, J. K. Sprafke, F. A. Leibfarth, C. J. Hawker, N. A. Lynd, *Macromolecules* **2012**, *45*, 3722–3731.
- 34 J. Yu, W. Wei, E. Danner, R. K. Ashley, J. N. Israelachvili, J. H. Waite, *Nat. Chem. Biol.* **2011**, *7*, 588–590.
- 35 H. Lee, N. F. Scherer, P. B. Messersmith, *Proc. Natl. Acad. Sci.* **2006**, *103*, 12999–13003.
- 36 K. H. Tan, R. Nishida, *J. Insect Sci.* **2012**, *12*, 1–74.
- 37 R. D. Crouch, *Tetrahedron* **2013**, *69*, 2383–2417.
- 38 J. Heo, T. Kang, S. G. Jang, D. S. Hwang, J. M. Spruell, K. L. Killops, J. H. Waite, C. J. Hawker, *J. Am. Chem. Soc.* **2012**, *134*, 20139–20145.
- 39 (a) J. K. Sprafke, J. M. Spruell, K. M. Mattson, D. Montarnal, A. J. McGrath, R. Pöttsch, D. Miyajima, J. Hu, A. A. Latimer, B. I. Voit, T. Aida, C. J. Hawker, *J. Polym. Sci., Part A: Polym. Chem.* **2015**, *53*, 319–326; (b) J. Nishida, M. Kobayashi, A. Takahara, *J. Polym. Sci., Part A: Polym. Chem.* **2013**, *51*, 1058–1065; (c) H. Watanabe, A. Fujimoto, A. Takahara, *J. Polym. Sci., Part A: Polym. Chem.* **2013**, *51*, 3688–3692; (d) R. Gu, W. Z. Xu, P. A. Charpentier, *J. Polym. Sci., Part A: Polym. Chem.* **2013**, *51*, 3941–3949.
- 40 (a) C. E. Hoyle, T. Y. Lee, T. Roper, *J. Polym. Sci., Part A: Polym. Chem.* **2004**, *42*, 5301–5338; (b) N. Gupta, B. F. Lin, L. Campos, M. D. Dimitriou, S. T. Hikita, N. D. Treat, M. V. Tirrell, D. O. Clegg, E. J. Kramer, C. J. Hawker, *Nat. Chem.* **2010**, *2*, 138–145.
- 41 J. D. White, J. J. Wilker, *Macromolecules* **2011**, *44*, 5085–5088.